Snake 모델에서의 개선된 Gradient Vector Flow: 캡쳐 영역의 확장과 요면으로의 빠른 진행

(Enhanced Gradient Vector Flow in the Snake Model: Extension of Capture Range and Fast Progress into Concavity)

조 익 환 † 송 인 찬 †† 오 정 수 †††
(Ik-Hwan Cho) (In-Chan Song) (Jung-Su Oh)
엄 경 식 †††† 김 종 효 †† 정 동 석 †††††
(Kyong-Sik Om) (Jong-Hyo Kim) (Dong-Seok Jeong)

요 약 Gradient vector flow(GVF) snake 또는 active contour 모델은 영상 분할에서 훌륭한 성능을 보여준다. 그러나 기존의 snake 모델에는 제한된 캡쳐 영역과 요면으로의 느린 진행과 같은 문제점들이 존재한다. 본 논문은 주변의 필드로부터 외부장(external force field)을 확장시키고 변형된 평탄화기법을 이용하여 확장된 필드를 정규화 함으로서 GVF snake 모델의 성능을 개선시키는 새로운 방법을 제시한다. 시뮬레이션을 위해 사용된 U자 모양 이미지에서의 결과는 제안된 방법이 좀 더 큰 캡쳐 영역을 갖고 기존의 GVF snake 모델에 비하여 요면으로 빠르게 진행하는 것이 가능함을 보여준다.

키워드 : Active contour, Gradient Vector Flow, 캡쳐 영역, 외부장

Abstract The Gradient Vector Flow (GVF) snake or active contour model offers the best performance for image segmentation. However, there are problems in classical snake models such as the limited capture range and the slow progress into concavity. This paper presents a new method for enhancing the performance of the GVF snake model by extending the external force fields from the neighboring fields and using a modified smoothing method to regularize them. The results on a simulated U-shaped image showed that the proposed method has larger capture range and makes it possible for the contour to progress into concavity more quickly compared with the conventional GVF snake model.

Key words : Active contour, Gradient Vector Flow, Capture range, Extension field

1. Introduction

The snake or active contour model that was first proposed by Kass[1] is widely used in many applications such as object segmentation [2], motion tracking[3], computer vision[4] and shape modeling [5]. Generally, there are two types of active contour models: the parametric active contour[1] and geometric active contour models[6-8]. This paper focuses on the parametric active contour model, which represents the curves and surfaces explicitly in their parametric forms during deformation. The traditional parametric active contour model is a curve $x(s) = [x(s), y(s)]$, $s \in [0,1]$ that moves through the spatial domain of an image to minimize the energy functional

† 학생회원 : 인하대학교 전자공학과
teddydino@inhaian.net
†† 비 회 원 : 서울대학교 병원 진단방사선과 교수
icsong@radcom.snu.ac.kr
kimjh@radcom.snu.ac.kr
††† 비 회 원 : 서울대학교 의학연구원
koorye@snuvh.snu.ac.kr
†††† 비 회 원 : (주)캐드임팩트 마케팅 대표이사
ksom@chol.com
††††† 비 회 원 : 인하대학교 전자공학과 교수
dsjeong@inha.ac.kr
논문접수 : 2005년 9월 2일
심사완료 : 2005년 11월 24일

$$E = \int_0^1 \frac{1}{2}\left[\alpha|\mathbf{x}'(s)|^2 + \beta|\mathbf{x}''(s)|^2\right] + E_{ext}(\mathbf{x}(s))ds \quad (1)$$

where α and β are weighting parameters that control the snake's tension and rigidity, respectively, and $\mathbf{x}'(s)$ and $\mathbf{x}''(s)$ denote the first and second derivatives of $\mathbf{x}(s)$ with respect to s.

The parametric active contour algorithm has two main difficulties. First, the initial contour must be set close to the real edge for a correct deformation. If the initial contour is set far from the real edge, it might converge into the wrong shape. Many methods were proposed to resolve this problem such as multi-resolution methods[9], pressure forces [10], and the distance potential method[11]. Second, it is difficult for the initial contour to progress into boundary concavities. Although several methods have been proposed, there is no satisfactory solution to this problem.

The GVF snake model proposed by Chenyang and Jerry showed successful results regarding these problems[12]. They defined the gradient vector flow field as the vector field $\mathbf{v}(x,y) = [u(x,y), v(x,y)]$, which minimizes the energy function

$$\varepsilon = \int\int \mu(u_x^2 + u_y^2 + v_x^2 + v_y^2) + |\nabla f|^2 |\mathbf{v} - \nabla f|^2 \, dxdy \quad (2)$$

In this equation, f is an edge map derived from the image and u_x, u_y and v_x, v_y are x or y directional derivatives of u and v. Parameter μ is a regularization parameter that controls the trade-off between the first and second terms. This variational formulation follows a standard principle, which smoothes the result when there is no data. Although their GVF snake model has a superior capture range and handles boundary concavity problems better than the previous methods, there are still limitations. Most important issue in conventional GVF is a limited capture range even if it is better than traditional snake model. Currently conventional GVF model has also limited capture range like traditional model. Since field including GVF field is made near edge, zero field increases as input image is simple. If initial contour locates in zero fields, it cannot move target position. Hence to make contour deform into target position regardless of initial location in image, fields must be distributed in entire image range.

Several methods to enhance the performance of GVF snake model have been suggested. Xu. And Prince. proposed Generalized Gradient Vector Flow (GGVF) in[13]. In [13], they two spatially varying weighting functions to solve concave problem while maintaining large capture range. Zeyun et al. proposed a Gradient Vector Diffusion (GVD)[14] algorithm. They reported a new type of anisotropic diffusion equation that not only provided a good estimate of the initial snakes but also generated an external force on each pixel in the image domain. Dan suggested a new external force field called the Simulated Static Electric Field (SSEF)[15]. However, there were difficulties in driving into a narrow concavity as a result of the weak forces.

Therefore, this paper proposes an enhanced GVF method using field extension and smoothing processes to solve a limited capture range and concavity problems associated with the conventional GVF snake model.

2. Proposed Method

2.1 Overall Scheme

Fig. 1 shows an entire block diagram of the proposed algorithm based on the GVF snake model to enhance its performance. First operation is to set initial contour for final segmented results. And GVF fields for input image are calculated by [12]. In generally, GVF field calculation consists of three steps; gradient edge map, GVF field calculation and iterative modification. In these steps GVF field is calculated using Equation (2) and mathematical approximation method. Finally using iterative modification steps, final GVF field for input image is obtained. In this paper, we call it pre-generated field for final extended field since the proposed method is cascaded next GVF field calculation step as post-processing perspective. The cascaded proposed method has 3 sub steps; thresholding of the pre-generated GVF field, extension of field and regularization process. After above processes, better vector field is obtained and then initial contour is deformed using it iteratively. Finally, contour deformation is stopped in according with predefined termination conditions.

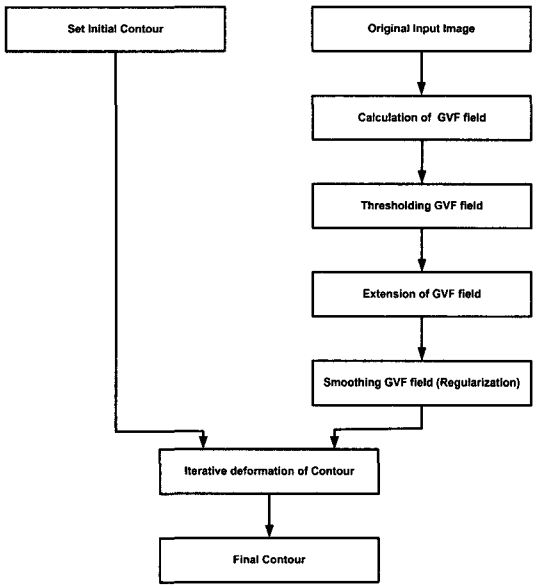

Fig. 1 Overall block diagram of the proposed algorithm

2.2 Extension of GVF field

The GVF snake model can overcome a limited capture range problem to some degree compared with the previous conventional snake models, but it is not considered to be a perfect solution. In general, a smoothing operation before the gradient operation of the original image has been used to extend the capture range. However, its real edges can be distorted because it can excessively distort the image. Hence, a precise contour could not be guaranteed. In addition, some parameters used in calculating a GVF field such as μ, α and β must be adjusted properly in order to resolve the initial contour problem. Consequently, the accuracy of contour deformation may decrease if more limited conditions are used.

This paper proposes a new algorithm to overcome the limited capture range problem by using the fact that a GVF field in a restricted range may be extended to the overall image range.

In some regions with non-zero GVF fields, they act as an external force of an active contour to guarantee the correct attraction of the contour into the real edge, but they cannot extend to other regions with no GVF field. If there is a path of external forces between the real edge and the initial contour, it may be attracted into the real edge despite the initial contour being far from the real edge. However, the undetermined external force of each point in the path were estimated from the fields already generated because there was no information that can be used to estimate the proper external forces in the regions with no GVF field. Fig. 2 represents the basic design for estimating the undetermined external force.

The initial contour was set far from the real edge in Fig. 2(a). The GVF snake algorithm generates a GVF field near the real edge and may have relatively wider capture range than the conventional snake models. However, there are still undetermined GVF fields between the edge and the initial contour. In order to correctly attract the initial contour into the real edge, there must be a continuous path that consists of several consecutive external force fields between them. Fig. 2(b) represents an estimated GVF field path from its pre-generated near real edge.

It is quite difficult and exhaustive to determine an optimal continuous point-by-point path. Therefore, in order to reduce the complexity of the algorithm, the GVF field was extended instead of determining the continuous path point-by-point. In order to make the contour move to a real edge, estimating each path for each point of the initial contour in the snake algorithm only might be sufficient.

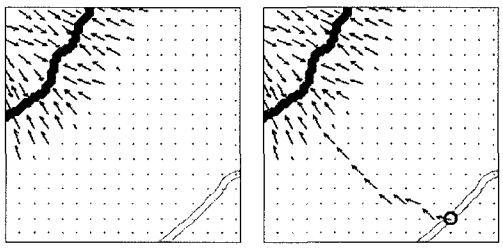

(a) (b)

Fig. 2 (a) Initial contour, real edge and its neighborhood GVF field, where the left top black line is a real edge and the right bottom gray line is an initial contour. (b) Estimated GVF field between the initial contour and the real edge in a path. The proposed method estimates the undetermined GVF fields between those previously generated and the initial contour

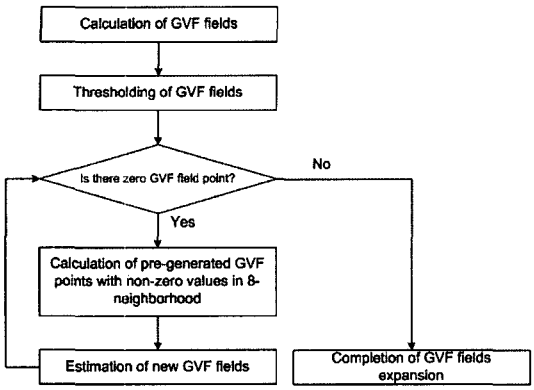

Fig. 3 Block diagram of GVF extension process

All points that have no GVF field values have new values through their extension. Fig. 3 represents the GVF extension algorithm in detail.

The undetermined GVF field values were estimated from pre-generated values. In this paper, pre-generated value or field is defined as the value by the initial general GVF field calculation or previous extension process. The pre-generated GVF fields were larger at regions close to the real edges relative to those far from them. In this paper, the pre-generated values were not modified. The following equations show how to estimate the new GVF fields in the points with a zero GVF field near the pre-generated fields. In this equation,

$$p_{x,new}(i,j)=\frac{w_{dist}}{N_{x,neighbor}(i,j)}\left[\sum_{n=-1}^{1}\sum_{m=-1}^{1}p_x(i+n,j+m)-p_x(i,j)\right], \quad if\ N_{x,neighbor}>0$$

$$p_{y,new}(i,j)=\frac{w_{dist}}{N_{y,neighbor}(i,j)}\left[\sum_{n=-1}^{1}\sum_{m=-1}^{1}p_y(i+n,j+m)-p_y(i,j)\right], \quad if\ N_{y,neighbor}>0 \tag{3}$$

$P_x(i,j)$ and $P_y(i,j)$ represent x- and y-directional GVF field values in location (i,j), $N_{x,neighbor}$ and $N_{y,neighbor}$ are the number of pre-generated GVF points with non-zero values in the 8-neighborhood pixels, w_{dist} is the distance weight (>1) and $p_{x,new}$ and $p_{y,new}$ are the new extended GVF field values.

In specific points with a zero value and non-zero pre-generated GVF fields in the 8-neighborhood pixels, their values were replaced using the pre-generated values in the 8-neighborhood pixels. Using this algorithm, all the points with zero GVF fields were iteratively extended from the whole pre-generated GVF field map. However, this extension process has several problems. The most critical is that the extended GVF field can decrease in the points far from the real edge where most of the pre-generated fields have very small values. Therefore, it is expected that the new extended GVF field may have a smaller value as the extension process proceeds. In order to resolve this problem, a threshold value, T, and a distance weight factor, w_{dist}, was used.

$$p_x=\begin{cases}p_x & if\ p_x\geq T\\ 0 & if\ p_x<T\end{cases}$$

$$p_y=\begin{cases}p_y & if\ p_y\geq T\\ 0 & if\ p_y<T\end{cases} \tag{4}$$

A threshold value, T, in the GVF field values and the distance weight factor prevented the extended value from reducing. This means that it is possible to dramatically deform the initial contour into a real edge even if it is set far from that the real edge. It is reasonable that the GVF field close to the real edge must be smaller than the others further away from the real edge because it can prevent the excessive deforming of the contour. In addition, the GVF field far from the real edges must be larger so that the contour deformation can be made more quickly.

Fig. 4 shows the result of GVF field extension process.

In a w_{dist} over 1, the GVF fields increase gradually as the field extension process iteratively continues. Therefore, the contour far from the real edge may

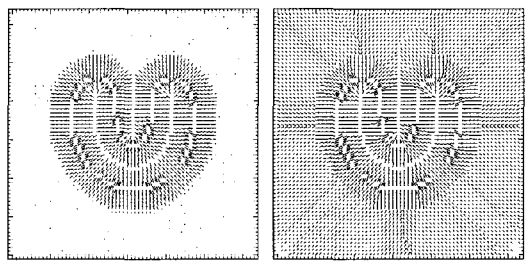

(a) (b)

Fig. 4. GVF field extension process. (a) Field map using the conventional GVF method. (b) Extended map using proposed method

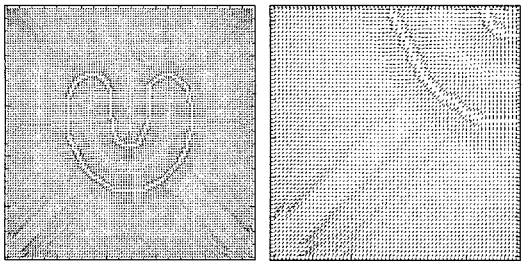

(a) (b)

Fig. 5 GVF field extension process using the distance weight factor. (a) Extended GVF field map of Fig. 4(a) using the distance weight factor over 1. (b) Magnified image of (a)

converge more rapidly. Fig. 5 shows the extended GVF fields using the distance weight factor.

2.3 Smoothing of GVF field

The main objective of the smoothing process for the extended GVF field is to help the contour to converge into the concavities faster.

In this paper, a simple smoothing mask, which is shown in Fig. 6, was applied to the extended GVF field map generated in the previous section.

$1/N_{NB}$ x

1	1	1
1	0	1
1	1	1

Fig. 6 A simple 3 x 3 smoothing mask, where NNB is the number of pixels with a non-zero GVF field in the 8-neighboring pixels

In the normalization factor, N_{NB}, the number of pixels with only non-zero values was used in order to prevent the smoothing values from decreasing at the region with a zero GVF field. Although the GVF field may extend to the whole regions using the proposed method, the zero field points might exist because their fields can cancel each other. The smoothing process was applied iteratively by just convolving the extended GVF field map with the proposed smoothing mask in Fig. 6 and stopped after the proper number of iterations according to the complexity of the image and the degree of its concaveness was reached. However, the image may require more iterations if it has a higher concavity and complexity.

3. Experiment Results

The proposed method based on the GVF snake model reported by Chenyang Xu and Jerry Prince was implemented on a platform of an IDL (Interactive Data Language, Research Systems, Inc) using a Pentium 4 1.6MHz PC. These experiments used a U-shape simulation image to represent the advantages of the wider capture range and the ability of the fast convergence into concavity in the proposed method relative to the classical GVF snake model. The U-shape image used in this paper has a 256×256 resolution and a gray level intensity. Fig. 7 shows the extended the capture range using the U-shape images with α=0.01, β =0.0 and μ=0.5 for GVF field calculation and γ (gamma)=5 and κ (kappa)=0.6 for the snake deformation. The threshold value for the pre-generated force field used before the main extension was 0.3. A classical GVF force field exists around the real edges and has a limited capture range, even though it is wider than the traditional snake models. Although several parameters in the GVF snake model might widen the capture range when used appropriately, it is difficult set the parameters properly. Moreover, it cannot extend the capture range to the whole region.

The convergence of the initial contour between the GVF snake model and the proposed method was tested. Fig. 7(b) and (d) show the force field maps generated by the classical GVF snake model and the proposed method, respectively, where the number of iterations for the smoothing process was 30. In the U-shape image, the initial contour was set very far from the real edge in order to compare the convergence of the initial contour.

Fig. 7(a) and (c) show the convergence of a contour using the classical GVF external force field and the extended external forces by the proposed method respectively. In Fig. 7(a), the initial contour in the GVF snake model could not converge into the real edge because there were no external forces close to the initial contour. However, the initial contour in the proposed method can converge into the real edge and progress into the boundary concavity if it is set close to the real edge, as

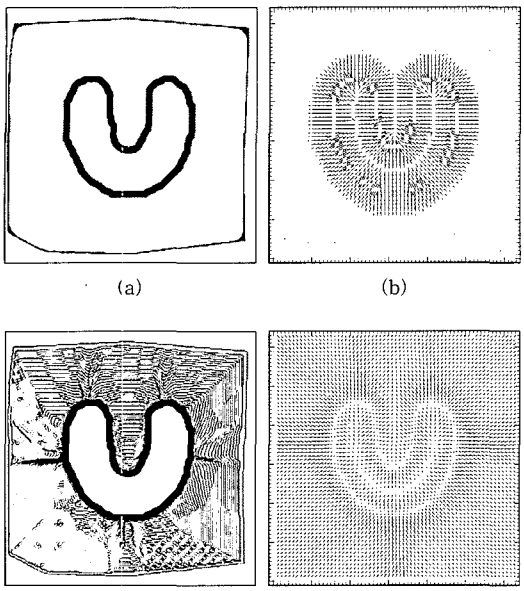

Fig. 7 The capture ranges in the U-shape image. A contour far from the real edge converges by using the extended external forces (d) by the proposed method in (c), but does not converge using the classical GVF external forces (b) in (a)

shown in Fig. 7(c) because of the existence of external forces close to the initial contour.

We validated the huge capture range of the proposed method through the real application, MR cardiac left-ventricular segmentation. The left-ventricle segmentation method used in this paper is based on [16]. The method from [16] preprocessed image using k-means clustering and merging and applied the GVF snake model to obtain final segmentation results. We used the proposed method instead of conventional GVF method to validate the powerfulness in capture range. Fig. 8(a) is the original MR cardiac left-ventricle image and we aim to obtain inner contour. K-means clustering and merging proposed in [16] simplified image such as Fig. 8(c). For experiments, we set the small initial contour in inner center position like Fig. 8(d). From GVF filed calculation and extension process, Fig. 8(e) and (f) were obtained. In this real application, it is very difficult for expert to set initial contour carefully for each image. Therefore drawing small closed-path in inner position may be very

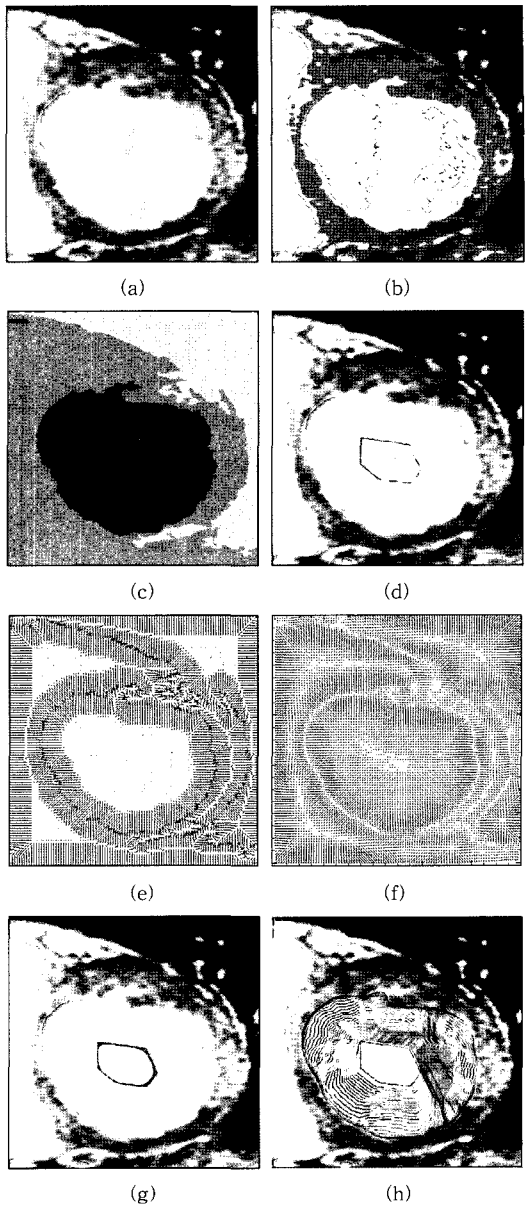

Fig. 8 Cardiac left ventricular segmentation results using conventional GVF and the proposed method. (a) is MR cardiac left ventricle image. (b) is k-means clustered image(number of clusters=4) of (a) and (c) is merged image (number of labels=3) of (b). (d) shows initial contour for segmentation of inner contour and (e) and (g) are GVF filed map and final segmentation result using conventional GVF method. (f) and (h) are GVF field map and final segmentation results using the proposed method

useful in reducing time and hand-work. In using conventional GVF method, final segmentation result is wrong because filed values for the propagation of contour exist mainly around real edges (Fig. 8(g)). However the proposed method using field extension and smoothing could support the widest capture range and segment inner boundary perfectly (Fig. 8(h)).

The proposed field extension method can widen the capture range regardless of the parameter value, μ (mu) that can be usually modified according to the noise level of the image and the capture range in the conventional GVF method. Fig. 7 shows the parameter independency of the proposed method relative to the conventional one. Fig. 9(a) and (b) show the GVF field using the conventional method and the proposed one with the same μ value (0.5). Through the field extension and smoothing process, (b) has a wider capture range than (a). Fig. 9(c) and (d) show the field generated using the same methods used in (a) and (b) with a different μ value (0.1). Since μ is smaller than (a), (c) shows a narrower capture range. However, (d) using the proposed method shows the capture range similar to (b) even if it uses a small μ value. Fig. 9(e) and (f) show the same experiment results using 10 iterations. Since the proposed method can widen the capture range with different parameter μ values and the number of iterations, the initial contour far from the real edge can converge into the correct ones such as Fig. 9(e) and (f).

In order to represent the advantage of the proposed method over previous methods for fast convergence into concavity, the number of iterations needed for the contour to converge into the concavity was evaluated.

Fig. 10(a) shows a 256 × 256 U-shape image and the initial contour. Fig. 10(b) and (c) show the magnified images of the classical and extended GVF force field maps according to the proposed method around the concavity, respectively. In the boundary concavity, the GVF snake model has few external forces toward the inside of the concavity even though it is better than any traditional snake model. However, in Fig. 10(c) of the extended force field map, many force fields face into the concavity,

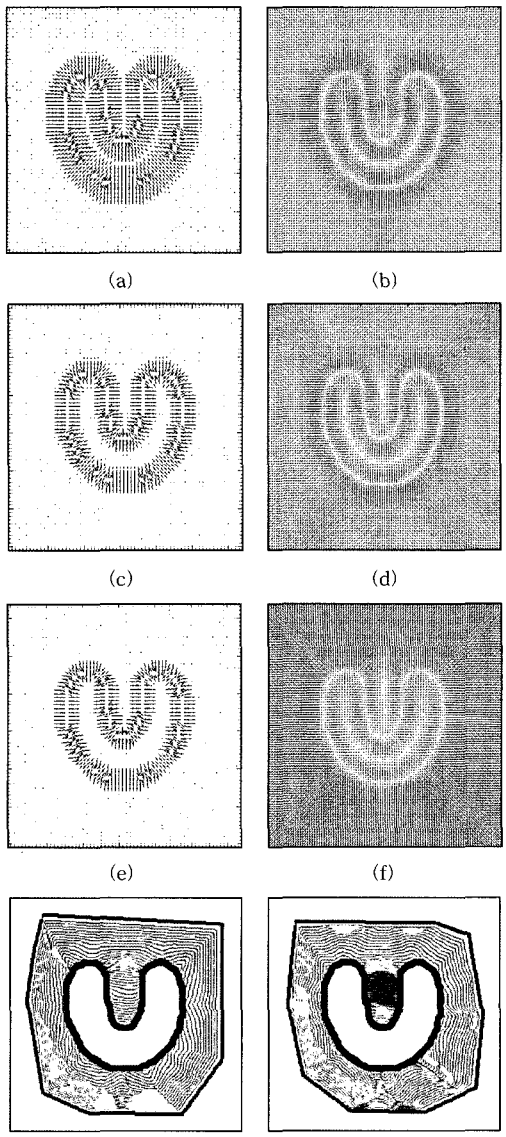

Fig. 9 Field extension process with the parameter values of μ and the number of iterations. (a), (c) and (e) show the GVF fields of the U-shape image using the conventional GVF method with different μ values ((a):0.5, (c): 0.1, (e):0.5) and the number of iterations ((a):30, (c):30, (e):10). GVF field (b), (d) and (f) using the proposed field extension method with the same μ values and the number of iterations with a wider capture range than (a), (c) and (e). (g) and (h) are the deformation results of the contour using (b) and (d).i

which can guide the contour into the concavity. Fig. 10(d), (e) and (f) show the convergence results of the contour using the GVF snake model after 18, 36 and 51 iterative deformations and Fig. 10(g), (h) and (i) show the convergence results using the extended external forces according to the proposed method after 18, 36 and 51 iterative deformations. In 18 iterative deformations, the two convergence results were similar. After 36 iterative deformations, the contour using the proposed method converged faster as the contour converged into the concavity than the classical GVF snake model. According to the proposed method, after 51 iterative deformations, the contour using the classical GVF snake model still converges into the concavity when the contour from the extended force field arrives at the

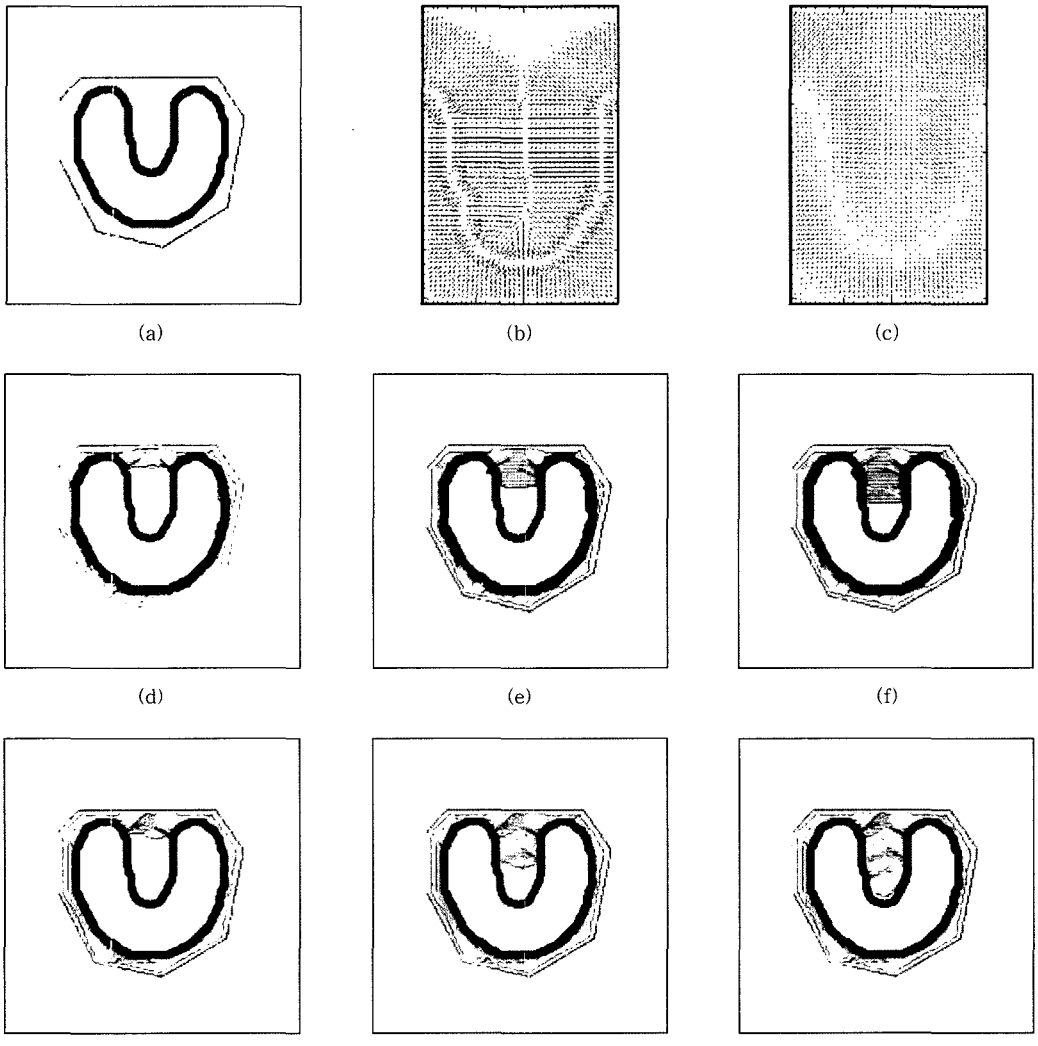

Fig. 10 Comparison of the convergence speed into the boundary concavity for the U-shape image. (a) The initial contour, (b) GVF external force field in the boundary concavity and (c) the extended force field by the proposed method in the boundary concavity. (d), (e) and (f) are the convergence of the contour using the GVF external force field after 18, 36 and 51 iterations. (g), (h) and (i) are the convergence of the contour using the extended external force field by the proposed method after 18, 36 and 51 iterations.g

end of the concavity.

4. Conclusion and Discussion

A GVF snake model is a very effective algorithm when applied to a deformable model and is widely used in many applications such as vision and medical imaging. However, it still has capture range and boundary concavity problems in actual applications. In this paper, the proposed method enhanced the performance of the GVF snake model by solving the capture range and boundary concavity problem by extending the GVF field and smoothing field.

In the capture range problem, the proposed method extended the limited external force field to the entire image. Therefore, it can converge into a real edge regardless of the location of the initial contour. The capture range of the classical GVF snake model may be controlled in accordance with several parameters such as the regularization parameter μ and the number of iterations[12]. However, in the proposed method, it could support the widest capture range regardless of several parameters used to generate the GVF force. Therefore, it can be independent of the parameters and it is more convenient to set the initial contour.

The proposed method also makes the contour progress into the boundary concavity more quickly than previous methods. In previous methods, the contour could not progress into the concavity because only a small field in the entrance of the concavity faces inside. Since most methods produce a field based on the image locality, the field usually faces the nearest edge[1,2,10]. Consequently, most of the fields inside the concavity usually point towards the direction normal to the concavity, and not in the tangent direction. The contour, which moved to the entrance of the concavity, may not progress inside if the direction of the field does not point to the inside direction. However, the proposed method considers the global characteristics of the image using the smoothing process of the field. The proposed field smoothing process did not consider just the nearest edges and thus resolved the local minimum problem. The iterative smoothing process made the overall shape of the field and helped the contour to progress more quickly. In the concavity, the iterative smoothing process combined the tangent directional field, which exists inside the concavity, with the normal directional field pointing to the nearest edge but not inside. Therefore, the final field pointed to the inside, which is in contrast to most previous methods.

Even if the proposed method supports advantages relative to the conventional GVF snake model, there are still problems that need to be solved. In the two processes of the proposed methods, the smoothing field process was applied iteratively. If the number of iterations is set properly, almost perfect results can be obtained. However, it is not easy to set the best number of iterations in many different kinds of images. As a general rule, a larger number of iterations are needed in images with many concavities. Therefore, more algorithms will be needed in the GVF snake model in order to obtain an optimal number of iterations so as to produce a better and more generalized performance. However, the computation time is expected to depend on the complexity of the image when processing the field extension.

Finally, the GVF snake model is a very useful algorithm that can be utilized in many real applications. Overall, a higher performance will be expected in many real applications when using the GVF snake model with the proposed method.

References

[1] M. Kass, A. Witkin, and D. Terzopoulos, "Snakes: Active contour models," *Int. J. Comput. Vis.*, vol. 1, pp. 321-331, 1987.

[2] F. Leymarie and M. D. Levine, "Tracking deformable objects in the plane using an active contour model," *IEEE Trans. Pattern Anal. Machine Intell.*, vol. 15, pp. 617-634, 1993.

[3] D. Terzopoulos and R. Szeliski, "*Tracking with Kalman snakes,*" in Active Vision, A. Blake and A. Yuille, Eds. Cambridge, MA: MIT Press, 1992, pp. 3-20.

[4] W. E. L. Grimson, *From Images to Surfaces: A computational study of the Human Early vision system.* Cambridge, MA: The MIT Press, 1981.

[5] D. Terzopoulos and K. Fleischer, "Deformable models," Vis. Comput., vol. 4, pp. 306-331, 1988.

[6] V. Caselles, F. Catte, T. Coll, and F. Dibos, "A geometric model for active contours," *Numer.*

Math., vol. 66, pp. 1-31, 1993.
[7] R. Malladi, J. A. Sethian, and B. C. Vemuri, "Shape modeling with front propagation: A level set approach," *IEEE Trans. Pattern Anal. Machine Intell.*, vol. 17, pp. 158-175, 1995.
[8] V. Caselles, R. Kimmel, and G. Sapiro, "Geodesic active contours," in *Proc. 5th Int. Conf. Computer Vision*, 1995, pp. 694-699.
[9] B. Leroy, I. Herlin, and L. D. Cohen, "Multi-resolution algorithms for active contour models," in *12th Int. Conf. Analysis and Optimization of Systems*, 1996, pp. 58-65.
[10] L. D. Cohen, "On active contour models and balloons," *CVGIP: Image Understand.*, vol. 53, pp. 211-218, Mar. 1991.
[11] L. D. Cohen and I. Cohen, "Finite-element methods for active contour models and balloons for 2-D and 3-D images," *IEEE Trans. Pattern Anal. Machine Intell.*, vol. 15, pp. 1131-1147, Nov. 1993.
[12] Xu. Chenyang, and J. L. Prince, "Snake, Shapes, and Gradient Vector Flow," *IEEE Transactions on Image Processing*, vol. 7, no. 3, Mar. 1998.
[13] Xu. Chenyang, and J. L. Prince, "Generallized Gradient Vector Flow External Forces for Active Contours," Signal Processing, vol. 71, issue. 2, Dec., pp. 131-139, 1998.
[14] Z. Yu and C. Bajai, "Image Segmentation Using Gradient Vector Diffusion and Region Merging," *Proceedings of the 16th International Conference on Pattern Recognition*, vol. 2, pp. 941-944, Aug 2002.
[15] Dan Yuan and Siwei Lu, "Simulated Static Electric Field(SSEF) Snake for Deformation Models," *Proceedings. 16th International Conference on Pattern Recognition*, vol. 1, pp. 11-15, Aug 2002.
[16] I.H. Cho, J.S. Oh, K.S. Om, I.C. Song, K.H. Chang and D.S. Jeong, "Preprocessing Effect by Using k-means Clustering and Merging Algorithms in MR Cardiac Left Ventricle Segmentation," *Journal of Biomedical Engineering Research*, vol. 24, pp. 55-60, Apr. 2003.

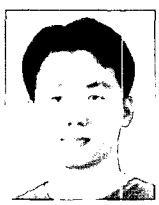

조 익 환

2000년 2월 인하대학교 전자공학과(공학사). 2002년 2월 인하대학교 전자공학과(공학석사). 2002년 3월~현재 인하대학교 전자공학과 박사과정 정보공학 전공. 관심분야는 의료영상처리, 워터마킹, 비디오 코딩, SVC

송 인 찬

1985년 2월 서울대학교 자연과학대학 물리학과 학사. 1989년 2월 서울대학교 대학원 물리학과 석사. 1996년 2월 서울대학교 대학원 미생물학과 박사. 1996년~1999년 서울대학교 의학연구원 방사선의학연구소 선임연구원. 2000년~현재 서울대학교 병원 전임강사. 관심분야는 MRI, DTI, 의료영상처리

오 정 수

1999년 2월 서울대학교 대학원 공과대학 전기공학부 학사학위. 2001년 2월 서울대학교 대학원 공과대학 협동과정의용생체공학전공 석사학위. 2005년 8월 서울대학교 대학원 공과대학 협동과정의용생체공학전공 박사학위. 2005년 9월~현재 [1]서울대학교 의학연구원 방사선의학연구소, [2]서울대학교 의과대학 해의학교실. 관심분야는 MRI, 의료영상처리, DTI, Brain Fiber Tracking

엄 경 식

1994년 2월 인하대학교 공과대학 전자공학과(공학사). 1996년 2월 인하대학교 대학원 전자공학과(공학석사). 2000년 2월 서울대학교 대학원 협동과정 의용생체공학전공(공학박사). 2000년 3월~2003년 2월 서울대학교 의학연구원 의용생체공학연구소 선임연구원. 2003년 3월~현재 ㈜캐드임팩트 대표이사. 관심분야는 인공 지능, 컴퓨터 보조 진단, 의료 영상 처리

김 종 효

1982년 서울대학교 공과대학 전자공학과 학사. 1994년 서울대학교 대학원 전자공학과 박사. 1995년~2001년 서울대학교 의과대학 방사선과학교실 조교수. 2001년~2002 하버드 의대 방문교수. 2002년~현재 서울대학교 의과대학 방사선과학교실 부교수. 관심분야는 의료영상 처리, CAD(Computer Aided Diagnostics), PACS

정 동 석

1977년 서울대학교 공과대학(학사). 1985년 Virginia Tech. (공학석사). 1988년 Virginia Tech.(공학박사). 현재 인하대학교 전자공학과 교수. 관심분야는 영상처리, 컴퓨터 비전, 비디오 압축 및 코딩